FINAL REPORT

ITOS VHRR ON-BOARD DATA COMPRESSION STUDY

NASA Contract NAS5-21940

Systems Analysis

1856 Elba Circle
Costa Mesa, California 92626

Report No. 75100

January 1975

Prepared by:
R.M. Gray
L.D. Davisson

Approved by:
Lee D. Davisson, PhD
President

ITOS VHRR ON-BOARD DATA COMPRESSION STUDY

BY

R. M. GRAY

L. D. DAVISSON

SYSTEMS ANALYSIS COMPANY

COSTA MESA, CALIFORNIA

January 1975

TABLE OF CONTENTS

LIST OF FIGURES

LIST OF TABLES

LIST OF FIGURES

ITOS VHRR ON-BOARD DATA COMPRESSION STUDY

Data compression methods for ITOS VHRR data have been studied for a tape recorder record-and playback application. A playback period of 9 minutes was assumed with a nominal 18 minute record period for a 2-to-1 compression ratio. Both analog and digital methods were considered with the conclusion that digital methods should be used. Two system designs were prepared. One is a PCM system and the other is an entropy-coded predictive-quantization (sometimes called entropy-coded DPCM or just DPCM) system. Both systems use data management principles to transmit only the necessary data. Both systems use a "medium capacity standard tape recorder" from specifications provided by the technical officer. The 10^9 bit capacity of the recorder is the basic limitation on the compression ratio. Both systems achieve the minimum desired 2 to 1 compression ratio. A slower playback rate (and hence bit transmission rate) can be used with the DPCM system due to a higher compression factor for better link performance at a given CNR in terms of bandwidth utilization and error rate. To achieve these gains more complex logic must be used. Further gains could be achieved by using a smaller tape recorder. The report is divided into two parts. The first part summarizes the theoretical conclusions of the second part and presents the system diagrams. The second part is a detailed analysis based upon an empirically derived random process model arrived at from specifications and measured data provided by the technical officer.

I Data Compression System Designs

1. Introduction

The presently existing ITOS very high resolution radiometer (VHRR) data utilization capability is highly restricted due to the maximum nine minute on-board analog tape storage capability. Much of the VHRR data is highly redundant, consisting of very flat or periodic segments which are amenable to sophisticated data compression processing techniques so that more than nine minutes of real time data can be stored at a reduced record speed while retaining a nine minute playback capability. A sample of the data output appears in figure*I.1.1. The data timing information appears in table *I.1.1. Figure I.1.1 and table I.1.1 together with digital tape samples provide the basis for the theoretical data model used in the data compression analyses and designs.

Data compression can be achieved through analog or digital methods. Analog methods were considered and discarded early in the study due to the overall trend toward digital methods in data communications and the attainability of practical data compression with digital methods.

Two digital tape recorders were used nominally in the study, the specifications for which were provided by the contract technical officer. These appear in tables I.1.2 and I.1.3 and are labelled "small capacity""and medium capacity" respectively and will be referred to as such subsequently. For the purposes of comparison, table I.1.4 presents the comparable specifications for the present ITOS analog tape recorder as provided by the contract technical officer.** It is seen that a size advantage is gained by using either digital recorder and a power and weight advantage is gained by the small capacity recorder. At the 18/9 minute nominal record/playback times the medium capacity and analog recorders appear to be about equal in power requirements. It will be shown that the small capacity recorder can not be used in this application due to the 10^8 bit capacity limitation but that the medium capacity one can be used with a large safety margin at the 2 to 1 compression ratio level.

---

*Reproduced from "Modified Version of the Improved TIROS Operational Satellite," by A. Schwalb NOAA TM NESS 35, dated April, 1972.

**Report of the Tape Recorder Action Plan Committee," NASA SP-307, dated March 21, 1972.

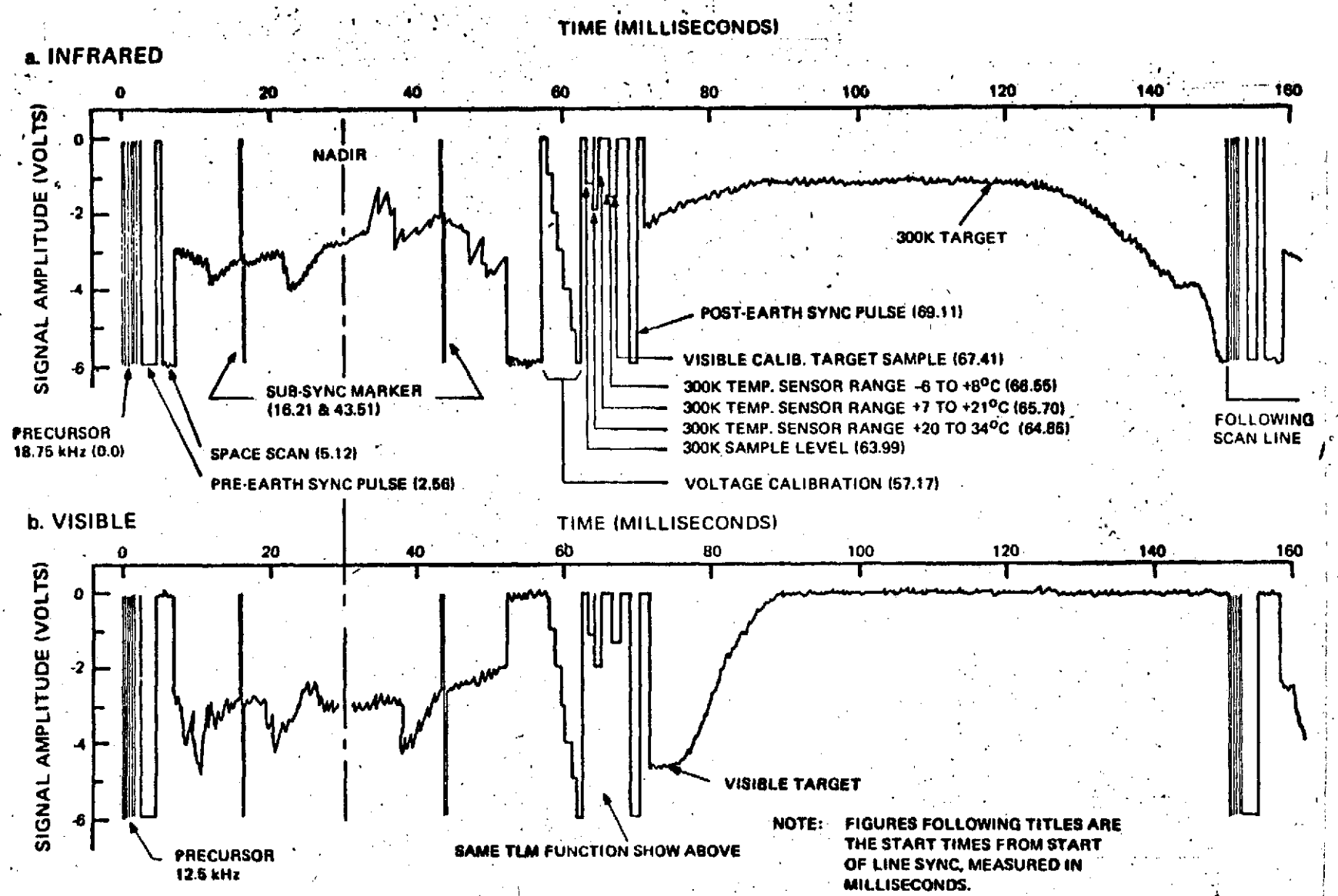

FIGURE 1.1.1 . VHRR Signals

Function	After Start of IR Precursor Counts*	Time (msec)	Duration Counts	Time (msec)	Signal Characteristics
Precursor IR	0	0	5.2	1.71	18.75 kHz square wave. 0 to 100% amplitude starts 72 ± 1° before nadir
Pre-earth Synchronisation signal					
Front Porch	521	1.71	256	0.85	Amplitude 0%
Sync Pulse	768	2.56	512	1.71	Amplitude 100%. Starts 65.8 ±1° before the nadir
Back Porch	1280	4.27	256	0.85	Amplitude 0%
Space scan	1536	5.12	Not clock controlled	2.08†	Amplitude 100% period varies with spacecraft altitude & attitude
Earth scan		7.20†	Not clock controlled	45.32†	Amplitude varies over range 0% to 100% (0% Hot, 100% Cold). Period varies from 43.68 msec @900 n.mi. to 48.64 msec @600 n.mi.
1st Sub-Sync marker	4864	16.21	16	0.05	Two level signal starting at 0% amplitude for ½ the period when switching to 100% for the remainder of the period
2nd Sub-Sync marker	13056	43.51	16	0.05	Same as 1st Sub-Sync marker
Space scan (post earth)	Not clock controlled	52.52	--	4.64†	Amplitude is undefined as signal may be influenced by the visible channel calibration target
Voltage Calibration	17152	57.17	1792	5.97	Seven levels increasing in amplitude from 0 to 100%. Zero level following 7th step.
Visible calibration	18944	63.14	256	0.85	Normal range when target is illuminated by sun is about 20% amplitude
Radiance calibration 300K target	19200	63.99	256	0.85	Amplitude about 20%. Varies with target's actual temperature

TABLE I.1.1. VHRR TIMING

Function	After Start of IR Precursor Counts*	Time (msec)	Duration Counts	Time (msec)	Signal Characteristics
Temperature Sensor 300K target (expanded range +20 to +34°C)	19456	64.85	256	0.85	For normal temperature range amplitude will be between 0 and 80%. (If the temperature is out of this range, the signal will either be 0 or between 85% and 100%)
Temperature Sensor (expanded) range +7 to +21°C)	19712	65.70	256	0.85	Same as above
Temperature Sensor (expanded range -6 to +8°C)	19968	66.55	256	0.85	Same as above
Post-earth Synchronization					
Front Porch	20224	67.41	1024	3.41	Amplitude 0%
Sync Pulse	21248	70.82	256	0.85	Amplitude 100%
Back Porch	21504	71.67	256	0.85	Amplitude 0%
End of IR scan	21760	72.53			
Precursor Vis	22523‡	75.00±1.00	512	1.71	12.50kHz square wave. 0 to 100% amplitude. Starts 72±10 before nadir
Pre-earth Synchronization Signal					
Front Porch	23035	76.78	256	0.85	Same as IR signal
Sync Pulse	23291	77.63	512	1.71	Same as IR signal
Back Porch	23803	79.34	256	0.85	Same as IR signal
Space scan (pre-earth)	24059	80.19	Not clock controlled	2.08†	Amplitude 0%. Period varies identically with IR signal

TABLE I.1.1 (cont)

Function	After Start of IR Precursor Counts*	Time (msec)	Duration Counts	Time (msec)	Signal Characteristics
Earth scan	Not clock controlled	82.27†	Not clock controlled	45.32†	Amplitude varies over range of 0% to 100%. (0% Black, 100% White). Period varies identically with IR channel.
1st Sub-Sync marker	27387	91.28	16	0.05	Same as IR signal
2nd Sub-Sync marker	35579	118.58	16	0.05	Same as IR signal
Space scan (post earth)	Not clock controlled	127.59	Not clock controlled	4.64†	Same as IR signal
Voltage calibration	39675	132.24	1792	5.97	Same as IR signal
Visible calib. target	41467	138.22	256	0.85	Same as IR signal
Radiance calibration 300°K target	41723	139.00	256	0.85	Same as IR signal
Temperature sensor (+20 to 34°C)	41979	139.93	256	0.85	Same as IR signal
Temperature sensor (+7 to +21°C)	42235	140.78	256	0.85	Same as IR signal
Temperature sensor (-6 to +8°C)	42491	141.64	256	0.85	Same as IR signal
Post-earth Synchronisation Signal					
Front Porch	42747	142.49	1024	3.41	Same as IR signal
Sync Pulse	43771	145.90	256	0.85	Same as IR signal
Back Porch	44027	146.76	256	0.85	Same as IR signal
Multiplex tolerance safety zone	44283	147.61	--	~2.39	
End of Scan		150.00			

*A count is one cycle of 300-kHz square wave.
†Spacecraft at 790 n.mi., 0° roll error, and nominal position for start of precursor
‡Nominal value for switchover from IR to Visible Scan. All following times assume that this switchover is nominal.

TABLE I.1.1 . (cont)

Table I.1.2

Small Capacity Standard Tape Recorder

Storage Capacity: 10^8 bits
Record/playback time: 2.62 minutes to 28 hours
Record/Playback rate: $\leq 6.4 \times 10^5$ bps
9 Minute playback rate: $\leq 10^8$ bits/540 sec = 1.9×10^5 bps
Size: 156 in^3
Weight: 10 lbs.
Power: $\leq$ 10w.
Cost: Unknown

Table I.1.3

Medium Capacity Standard Tape Recorder

Storage Capacity: 10^9 bits
Record/playback time: 31/8 minutes to 26 2/3 hours
Record/Playback rate: $\leq 5.12 \times 10^6$ bps
9 minutes playback rate: $\leq 10^9$ bits/540 sec. = 1.9×10^6 bps
Size: 468 in^3
Weight: 28 lbs.
Power: 10 to 40 watts
Cost: Unkown

Table I.1.4

ITOS Analog Tape Recorder

Size: 1200 in^3
Weight: 18.7 lbs.
Power: 19.8 w. (record), 16.1 w. (Playback)
Cost 200K

The detailed theoretical analysis appears in section II of this report. For analytical purposes the signal was assumed to be a uniform random variable on the [-6, 0] volts range shown in figure I.1.1 and to be sampled at 10^5 samples/sec (1.43 times the Nyquist rate for a 35 khz nominal data cutoff frequency. Using these assumptions and a uniform quantizer, the signal-to-noise ratio was calculated as a function of the bits of quantization (table II. 3.1).

The number of bits of quantization times the sampling rate defines the required recording rate for a pulse code modulation (PCM) system which stores and transmits the bit stream without encoding. For a 2-to-1 compression ratio, the playback rate is then twice that number. The required total recorder capacity in bits is 540 (9 min x 60 sec/min) times this rate. From tables I.1.3 and II. 3.1 it is seen that the medium capacity recorder can be used at quantization levels up to around 8 bits (48 db SNR) for a 2 to 1 compression ratio (18 minutes of data). Higher compression can be attained at lower quantization levels.

Further compression can be attained by data processing operations. The data are fairly inactive except during the earth scan. By transmitting only the earth scan and single values for the calibration-temperature data instead of long steps, approximately 40% of the digitized values are removed- a 40% reduction in average bit rate. Thus at 8 bits quantization, from table I.1.3, 10^9 bits/(8 bits x 60% x 10^5 samples/sec) = 2080 sec. or 35 minutes of data can be stored on the medium capacity recorder. The small tape recorder, on the other hand, can hold only 3.5 minutes at 8 bits quantization. Only at 1 bit quantization is the 2-to-1 compression ratio achieved- a quantization of no practical use.

From empirical studies and the theoretical results of section II of this report, in the 6-8 bit quantization range, about 3 more bits can be removed through entropy coded prediction-quantization (sometimes called differential pulse coded modulation (DPCM). In this scheme the difference is encoded by a variable length code between each successive value and its predicted value based upon past encoded values. Using this factor, at 8 bits quantization, 10^9 bits/((8-3) bits x 60% x 10^5 samples/sec) = 3333 sec. or 55 minutes of data can be stored on the medium capacity recorder. The small tape recorder, on the other hand can hold only 5.5 minutes of data. Only at impractically low levels of quantization can the small capacity tape recorder be used. Hence, it is recommended that the medium capacity tape recorder be used. It is clear that a substantial margin of storage could be used to store and replay more than 18 minutes of data if sufficient transmission channel capacity is available on playback. Alternately a smaller recorder, between those of figure I.1.2 and I.1.3 could be designed. It is clear in either case that the DPCM system requires a lower transmisssion rate and/or total capacity for a given compression ratio.

3. System Designs

Based upon the considerations given in the last section, two systems are recommended - a PCM system and a DPCM system. The PCM system is a subsystem to the DPCM system. Block diagrams of the two systems appear in figures I. 3. 1 and I. 3. 2. Both systems use the medium capacity tape recorder for a weight penalty of 9. 3 lbs. with a size gain of 732 in ^{3} over the ITOS analog recorder (see tables I. 1. 2 and I. 1. 3). Power requirements seem roughly equivalent.

The earth scan data are digitized by the A/D under control of the VHRR clock. The digitizing starts after a fixed delay from the start of scan so that only the earth data are included. The controller controls the insertion of the digitized values into the memory buffer and the output to the tape recorder. As the input rate is not constant, the controller also insures a constant output rate to the tape recorder and time multiplexes in the telemetry and calibration values. On command the recorder plays back the stored values at an increased rate over the record speed, the speed depending on the desired compression ratio.

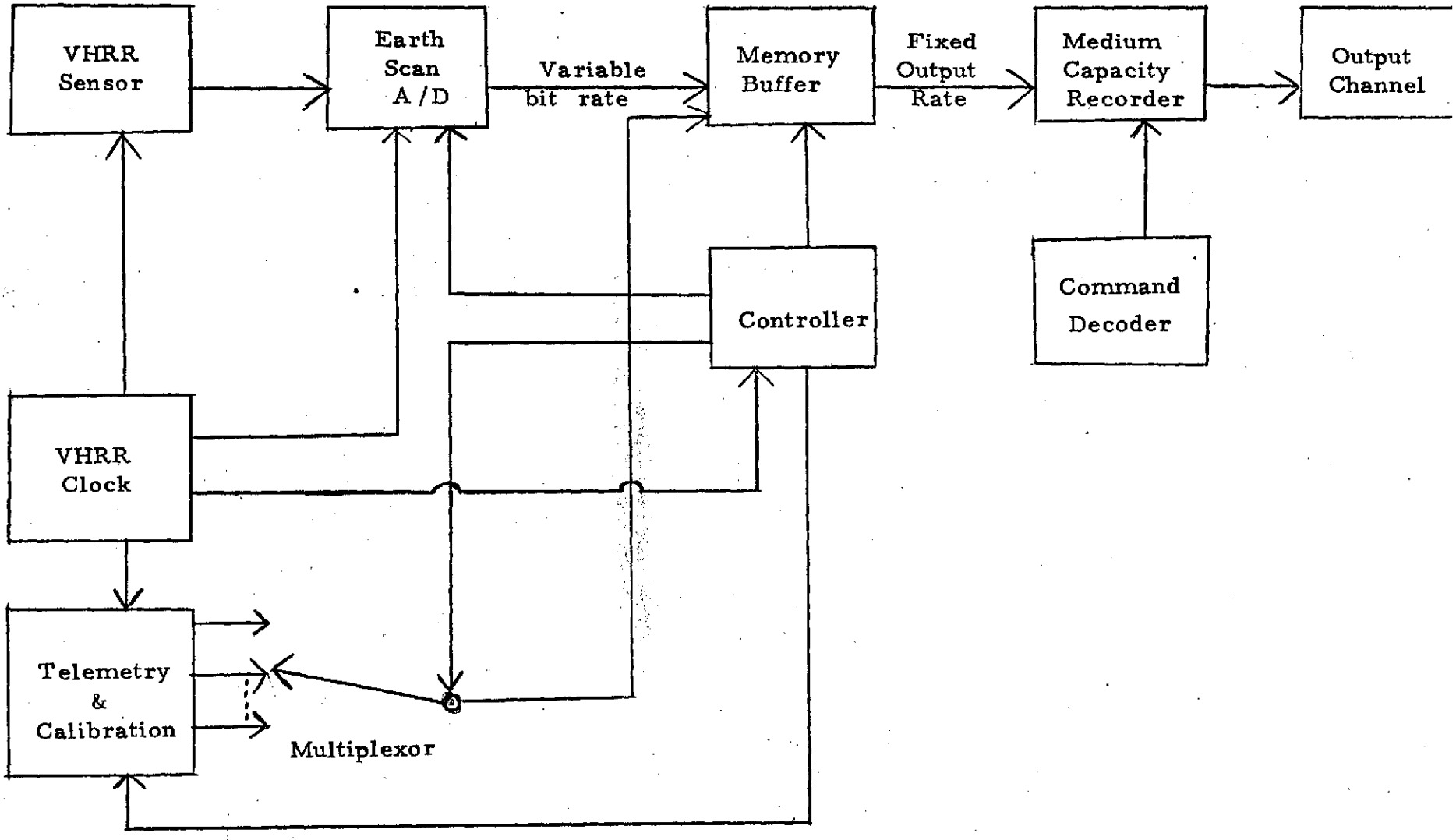

Figure I. 3.1 PCM System

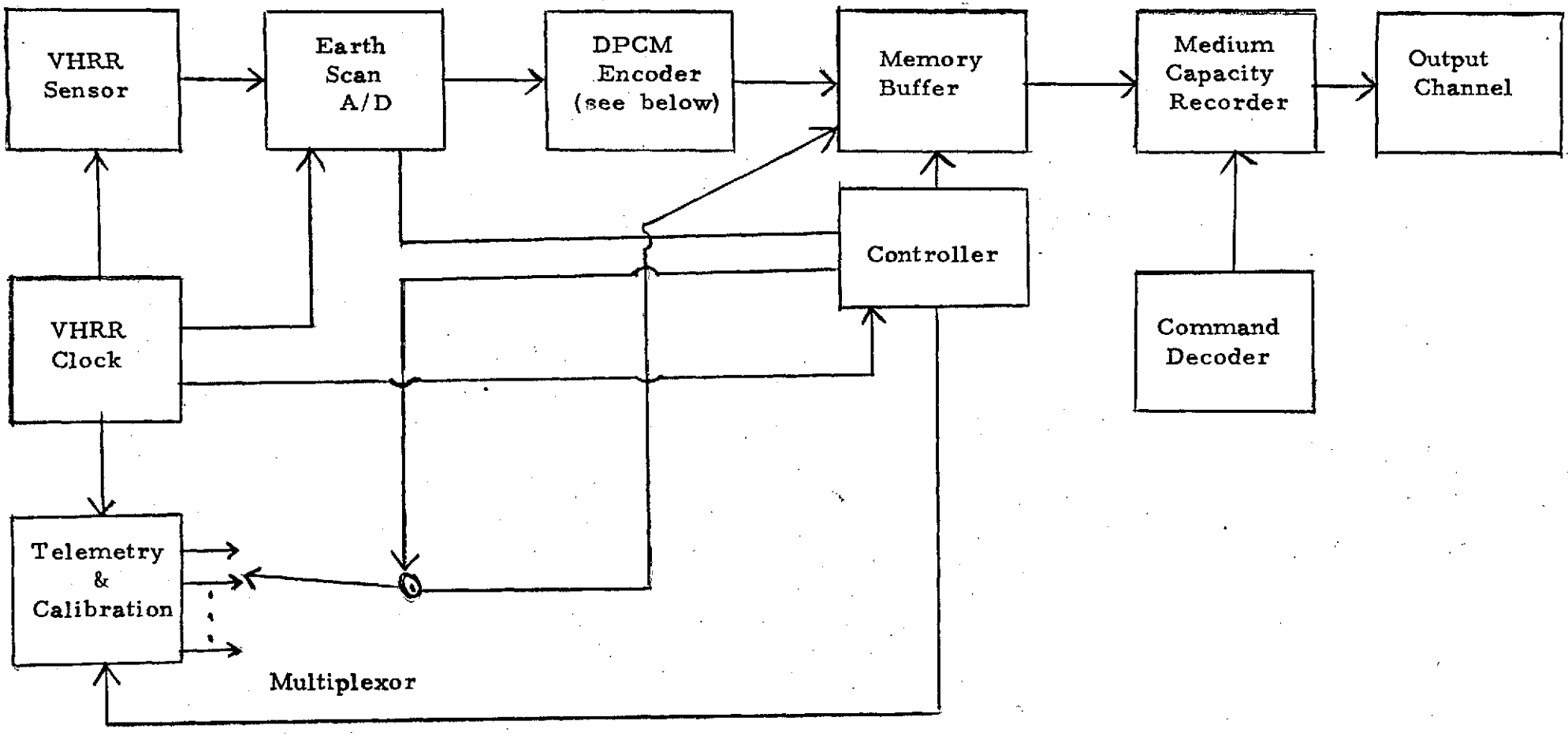

A Simple DPCM Encoder

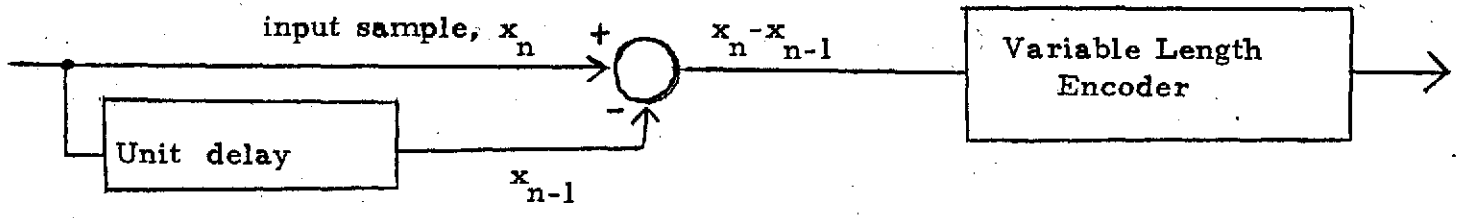

Figure I. 3. 2 DPCM System

II. Theoretical Analysis

1. Introduction

This section of the report presents the theoretical considerations involved in the choice of a data compression system. A theoretical data model is developed based upon empirical measurements and specifications from VHRR data provided by the GSFC technical officer. The data model is then used to analyze the performance of data compression algorithms in terms of required data rate and distortion, measured by mean squared error (signal-to-noise ratio).

2. Data Model

The source data to be compressed is assumed to be a "composite" or "switched" source consisting of four subsources. To characterize the composite source we describe each subsource and the amount of time spent in each.

Source 1: VHRR data with the satellite facing earth

Source 2: VHRR data with the satellite facing space

Source 3: Precursors

Source 4: Synchronization and Calibration data

Source 1: The earth VHRR data (the main data of interest) is modelled as a random process. In order to well approximate the data and yield a tractable model the random process model is assumed to satisfy the following:

i) The process is stationary and ergodic so that calculated ensemble averages will agree well with measured sample averages.

ii) The alphabet (range) of the data is the interval $[-6, 0]$ volts as in figure I.1.1.

iii) The marginal probability density is uniform on an interval of width $\lambda \leq 6$ volts.

iv) The data is highly correlated over short times. In particular, at the sampling frequency chosen to safely surpass the Nyquist rate the correlation coefficient is on the order of .85 - an empirically determined quantity.

v) The power spectral density falls off fairly rapidly. In particular, the 3db down frequency is a few khz and the power spectral density is negligible at 35kHz, say 20dB down from its maximum value.

An added assumption that is mathematically desirable and well matches the data is the following:

vi) The process is a Markov process.

A final, less precise assumption that is often adopted is the following:

vii) The second order properties (transition probabilities, covariance, power spectral density) should be approximately Gaussian. In particular, the covariance function should be well approximated by an exponential, the form of that of a Gauss-Markov source.

A model meeting all of these requirements is a Wiener process between reflecting barriers at $-\lambda$ and 0. In other words, if y(t) is a Wiener process, than the reflected process x(t) is defined as

$$x(t) \stackrel{\Delta}{=} -|y(t) - 2k\lambda|$$

where k is such that

$$-|y(t)-2k\lambda| \epsilon [-\lambda, 0]$$

If the Wiener process has parameter or incremental variance σ^2, then the transition probability density function is given by the "folded" Gaussian density

$$f_{x(t+\tau)|x(t)}(y|x) =$$

$$\sum_{k=-\infty}^{\infty} \frac{e^{\frac{-(y-x+2k\lambda)^2}{2|\tau|\sigma^2}}}{2\pi\sigma^2|\tau|} + \frac{e^{\frac{-(y+x+2k\lambda)^2}{2|\tau|\sigma^2}}}{2\pi\sigma^2|\tau|}$$

$$x, y \ \epsilon [-\lambda, 0] \qquad (2.1)$$

The random process $\{x(t);\ t \ \epsilon(-\infty, \infty)\}$ specified by

$$f_{x(t_1), \ldots, x(t_n)}(x_1, \ldots, x_n)$$

$$= \prod_{i=1}^{n} f_{x(t_{i+1})|x(t_i)}(x_{i+1}|x_i)\, f_{x(t_1)}(x_1)$$

where

$$f_{x(t_{i+1})|x(t_i)}$$

is given by 2.1 and

$$f_{x(t_1)}(x_1) = \lambda^{-1}, \quad x \in [-\lambda, 0]$$

is easily demonstrated to specify a stationary ergodic Markov process with uniform marginals. Thus the above model satisfies requirements (i), (ii), (iii), and (vi). To satisfy (iv) we must choose σ^2 to yield the desired covariance coefficient. Since we demand that frequencies up to 35kHz be reconstructed and do not care about power at higher frequencies, the Nyquist rate is 70kHz. To be both conservative and convenient we choose a sampling frequency of 100kHz= 10^5 samples per second. We require that

$$r \triangleq \rho_x(10^{-5}) = \frac{K_x(10^{-5})}{K_x(0)} = .85$$

where

$$K_x(\tau) \triangleq E\{(x(t) - \overline{x(t)})(x(t+\tau) - \overline{x(t+\tau)})\}$$

is the covariance function. It can be shown from (2.1) that

$$\rho_x(\tau) = \frac{K_x(\tau)}{K_x(0)} = \frac{96}{\pi^4} \sum_{n=0}^{\infty} \frac{e^{-\frac{1}{2}\frac{\sigma^2}{\lambda^2}\pi^2|\tau|(2n+1)^2}}{(2n+1)^4} \qquad (2.2)$$

For $\sigma/\lambda = 55.4$, $r = .85$, the desired covariance coefficient. To consider power spectral density we take the Fourier transform of the covariance function rather than the correlation function to avoid problems with the nonzero mean. It follows from (2.2) that the normalized spectral density is

$$\frac{S_x(f)}{S_x(0)} = \frac{960}{\pi^6} \sum_{n=0}^{\infty} \frac{(2n+1)^{-2}}{(2n+1)^4 + \left(\frac{4\lambda^2}{\sigma^2\pi} f\right)^2} \qquad (2.3)$$

At $f = 2400$ Hz, $S_x(f)/S_x(0) \tilde{=} 1/2$ and hence the 3db frequency, $f_{3dB} \tilde{=} 2400$ Hz. Furthermore, $S_x(35\times10^3)/S_x(0) = .0047$ so that the power spectral density is down 23dB at 35kHz and hence condition (v) is met.

Turning to assumption (vii) we note that the covariance coefficient of (2.2) is well approximated by its first term:

$$r_x(\tau) \cong \frac{96}{\pi^4}\exp\left[-\frac{1}{2}\frac{\sigma^2}{\lambda^2}\pi^2|\tau|\right] \qquad (2.4)$$

The approximation is quite good for moderate to large τ. Even for $\tau = 10^{-5}$, the first term approximation yields .847 while $\rho_x(10^{-5}) = .85$. Thus the covariance of x(t) is well approximated by the exponential form of a Gauss Markov covariance function. Next consider the transition density of (2.1). Approximating this sum by only one term would not provide a good approximation because the first term would approximate a Wiener process with resulting covariance coefficient $r = 1$ when in fact $r = .95$ by calculation. A better approximation is obtained by approximating $f_{x(t+\tau)|x(t)}$ by a Gaussian conditional density with the same second moments, that is,

$$f_{x(t+\tau)|x(t)}(y|x) \cong \frac{1}{2\pi(1-r^2)\sigma_x^2}\exp\left\{\frac{1}{2(1-r^2)\sigma_x^2}[(y-\bar{x})-r(x-\bar{x})]^2\right\} \qquad (2.5)$$

where $\bar{x} = Ex(t) = -\lambda/2$,

$$\sigma_x^2 = E\{(x(t) - \bar{x})^2\}$$

$$= \lambda^2/12$$

$$r = .85$$

To justify this approximation we note that it yields a conditional variance of

$$\sigma^2_{x(t+\tau)|x(t)=x} \cong \sigma_x^2(1-r^2) \cong .023\lambda^2$$

regardless of x. The expected value of the actual conditional variance can be shown to be

$$E\{\sigma^2_{x(t+\tau)|x(t)}\} = \sigma_x^2(1-\rho_x(2\tau)) \qquad (2.6)$$

Evaluating (2.6) using (2.2):

$$\rho_x(2 \times 10^{-5}) = .729$$

and hence

$$E\{\sigma^2_{x(t+\tau)|x(t)}\} = .023\lambda^2$$

Thus for the true model, $\sigma^2_{x(t+\tau)|x(t)}$ is a random variable (dependent on the value of x(t)) with expected value $.023\lambda^2$. For the Gaussian approximation the conditional variance $\sigma^2_{x(t+\tau)|x(t)}$ does not depend on x(t) and has the same value.

The fact that $E\{\sigma^2_{x(t+\tau)}\} = .023\lambda^2$ indicates that the variance is usually small in comparison with λ and hence the transition density should be fairly symmetric about its mean and fairly bell shaped for most x except those near the edges. Thus the approximation of (2.5) should be quite accurate except when $x = \lambda$ or 0, a relatively rare occurence.

The fraction of time spent in this subsource is roughly $2x(45.32)/150 \tilde{=} 60\%$.

Source 2: When looking at space the data is relatively constant at some unknown value. In particular, the large jumps visible during the earth scan do not appear. Thus this source can be modeled as a very slowly varying stationary drift process a(t) (roughly constant over at least 10ms intervals) with a small added random component $\delta(t)$. Let the subsource $w(t) = a(t) + \delta(t)$. From the observed data, $\delta(t)$ never changes by as much as 5v/m. s., that is,

$$Pr[(w(t+1m.\,s.)-w(t)\ |\geq 5] = Pr[\,|\delta(t+1m.\,s.)-\delta(t)|\geq 5] \tilde{=} 0$$

and hence since there are 100 samples per m. s.

$$Pr[|\delta(t+\tau)-\delta(t)|\geq .05] = 0 \qquad (2.7)$$

Because of this slow variation w(t) is relatively easy to compress and (2.1) is a sufficient characterization of the process. The subsource w(t) is in effect a fraction $[2.08 + 4.64]/150 = 4\%$ of the time.

Source 3: The precursors z(t) can be modeled as stationary square waves with frequency less than 18.75 k Hz. The only required characteristics are that the minimum time between jumps: $(18.75 \times 10^3)^{-1} = 5.3 \times 10^{-5} \geq 5\tau$, where τ is the sampling period, and that the crossing time is a uniform random variable (from the point of view of the compression system). The latter fact makes the square waves stationary. The fraction of time for this subsource is $2(1.71)/150 = 2\%$.

Source 4: This subsource includes the pre and post earth synchronization, the voltage, visible, and radiance calibration, and the temperature sensor data. We do not include the sub-synch markers of the earth scan in this source, but instead

consider them as simply rare events in the earth scan (the data compression device will locate and compress them as such). This source consists of stationary step functions with jumps no closer than .85 m. s. = 85 τ. The jumps when they occur may be any value between [-6, 6]. We assume a uniform distribution for jumps. This source is in effect a fraction

$$(1-.6-.04-.02) = 34\%$$

of the time.

To summarize, the data model, say v(t), appears as below:

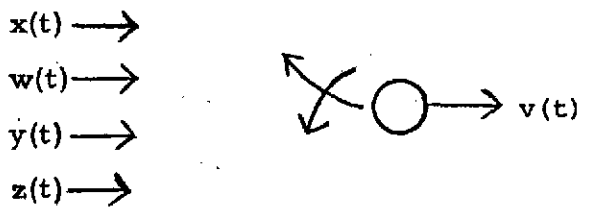

Switch position a deterministic time function.

We assume the four subsources are independent of each other and that the "starting time" of the switch sequence is uniformly distributed over [0, 150m. s.] so that v(t) is a stationary composite source. Furthermore, the marginal density for v(t) is approximately uniform and hence Ev(t) =v = -3, σ_v^2 =3.

3. Quantization and PCM

In this section we study the rate/distortion tradeoff from simple A/D conversion using binary pulse code modulation. Let R be the quantizer rate in bits per symbol, that is, each of the 10^5 samples per second is uniformly quantized using 2^R levels. Since $v_n \triangleq v(nt)$ is uniform, uniform quantization is optimal in the sense of minimizing distortion. For a range λ=6, rate R, and uniformly distributed v_n the quantization error is well known to be

$$E\{(x(nt)-q(x(nt)))^2\} = \epsilon_q^2 = \frac{(\lambda 2^{-R})^2}{12} = 3 \cdot 2^{-2R} \qquad (3.1)$$

Define the signal-to-quantization noise ratios as

$$SNR = \sigma_v^2 / \epsilon_q^2 = 2^{2R}$$

where the signal variance rather than power is considered to eliminate the nonzero mean. In decibels this is

$$\text{SNR} = 10 \log_{10} (\sigma_v^2 / \overline{\epsilon_q^2}) = 20R \log_{10} 2 \cong 6R \text{ db} \qquad (3.3)$$

The actual data transmission rate is R^* symbols per second = $R/T = R \times 10^5$ bits per second (6ps). Table II.3.1 summarizes the rate/distortion tradeoff for simple PCM.

Table II. 3. 1. Rate vs SNR for PCM

R	R^*	$\overline{\epsilon_q^2}$	SNR (db)
0	0	3	0
1	1×10^5	3/4 = .75	6
2	2×10^5	3/16 = .988	12
3	3×10^5	3/64 = .047	18
4	4×10^5	3/256 = .012	24
5	5×10^5	$3/1024 = 2.92 \times 10^{-3}$	30
6	6×10^5	$3/4096 = 7.32 \times 10^{-4}$	36
7	7×10^5	$3/16384 = 1.83 \times 10^{-4}$	42
8	8×10^5	$3/65536 = 4.58 \times 10^{-5}$	48

R = bits/sample

R* = bits/sec

$\tilde{\epsilon}_q^2$ = avg. quantization noise power

Suppose the design requirement for compressed data is to be equivalent in quality to 6 bit PCM or SNR = 36 db. Thus in any compression system producing an approximation v_n^* to v_n we require that

$$E\{(v_n - v_n^*)^2\} \leq 7.32 \times 10^{-4}$$

order is to playback data at twice the recording rate, the required bit rate of a tape recorder is thus $2 R \times 10^5$ bps. Thus for 36 db a 1.2×10^6 bps tape recorder is required if standard PCM is used. This is well within the range of the medium standard satellite tape recorder with 1.9×10^6 bps but is much greater than the rate of the lighter weight small standard satellite tape recorder with capacity 1.9×10^5 bps. If the small tape recorder is to be used, therefore, approximately 6:1 further compression would be required.

As a final note, nothing can be gained by noiseless coding the PCM data using a Shannon-Fano or Huffman code since the entropy of the uniformly quantized data $H(q(v_n)) = R$ since the v_n are uniformly distributed. Further gains($\approx$40%) could be achieved, however, by separating the earth scan data from the other, slowly varying data.

4. Predictive Quantization

In a predictive quantization scheme we transmit quantized error samples between the actual signal value and a prediction of the signal value. It is easily shown that one step linear prediction is nearly optimal for the x(t) subsource and hence we consider only simple linear prediction. If slight improvement is desirable, it is not clear whether two step linear prediction or the first two terms of the optimal nonlinear estimate is superior.

We shall design the compression scheme primarily for the most random subsource x(t), but we shall see that it works quite well on the composite source v(t).

Given the discrete-time process $x_n = x(nt)$ with $r = \rho_x(t) = E\{(x_n - \overline{x_n}) \cdot (x_{n-1} - \overline{x_{n-1}})\} / \sigma_x^2$, the optimal one-step linear predictor is given by

$$\hat{x}_n(x_{n-1}) = r\, x_{n-1} + \overline{x_n}(1-r) = r\, x_{n-1} - \frac{\lambda}{2}(1-r)$$

Define the error sequence $\epsilon_n = x_n - \hat{x}_n(x_{n-1}) = x_n - r\, x_{n-1} + \lambda/2\,(1-r)$ and note that $\epsilon_n = 0$ and $\sigma_{\epsilon_n}^2 = \sigma_\epsilon^2 = \sigma_x^2(1-r^2)$. We have by rearranging terms that

$$x_n = \sum_{k=-\infty}^{n} \epsilon_k r^{n-k} - \frac{\lambda}{2} \tag{4.1}$$

so that the error sequence determines the data sequence. We note that (4.1) is essentially an asymptotic or steady-state equation assuming the prediction to be done starting with the remote past without periodic initialization as is frequently used in practice.

The sequence $\{\epsilon_n\}$ has two advantages over the original data sequence from the standpoint of data compression. First, the marginal density for ϵ_n is more "bunched" since $\sigma_\epsilon^2 = \sigma_x^2(1-r^2) < \sigma_x^2$. This allows for further compression using either noiseless coding of the quantized error to take advantage of the reduced entropy or by non-uniform quantizing matched to the error sequence. Secondly, the error sequence is less correlated than the data sequence so that single symobl compression is nearly optimal. The decreased correlation follows, for example, since

$$|E(\epsilon_k \epsilon_{k+1})| = |(1+r^2) K_x(\tau) - r[K_x(0) + K_x(2\tau)]|$$

$$= \sigma_x^2 [r^3 - r\rho_x(2\tau)] \cong \sigma_x^2 (r^3 - r^3) = 0.$$

We note that if $\{x_n\}$ was actually Gauss-Markov with parameter r, then $\rho_x(2\tau) \equiv r^2$ and the above expression is exactly zero.

The preceeding discussion motivates the following system

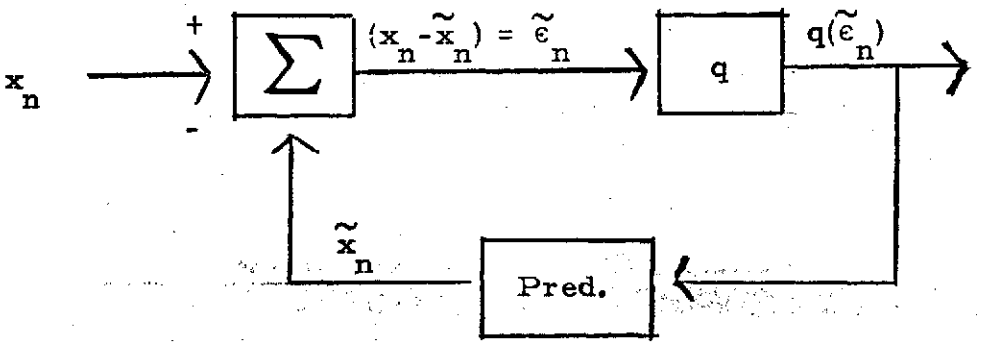

Encoder

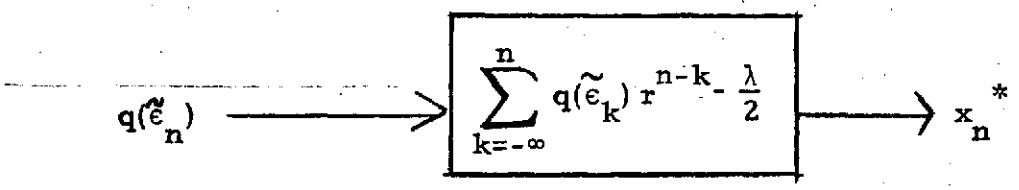

Decoder

Figure II. 4. 1

that is, we have simply replaced the errors ϵ_n by the quantized error sequence $q(\tilde{\epsilon}_n)$. The prediction is based on the quantized errors

$$\tilde{x}_m = r[x_{m-1} + \frac{\lambda}{2}] - \frac{\lambda}{2}$$

$$= \sum_{k=-\infty} q(\epsilon_k) r^{n-k} - \frac{\lambda}{2} \qquad (4.2)$$

so that

$$x_m^* = \tilde{x}_m + q(\tilde{\epsilon}_m)$$

is the approximation process. The average distortion is

$$E\{(x_n - x_n^*)^2\} =$$

$$E\{[(\tilde{x}_n + \tilde{\epsilon}_n) - (\tilde{x}_n + q(\tilde{\epsilon}_n))]^2\}$$

$$= E\{(\tilde{\epsilon}_n - q(\tilde{\epsilon}_n))^2\} \qquad (4.3)$$

since $x_n - x_n^* = \tilde{\epsilon}_n - q(\tilde{\epsilon}_n)$. That is, the data distortion equals the quantization distortion in the error sequence. It is often assumed that for sufficiently fine quantization, ϵ_n is probabalistically similar to the sequence $\tilde{\epsilon}_n$. The complicated feedback relation makes exact analysis difficult, but we can obtain a good approximation found as follows: We have

$$\epsilon_n = x_n - (rx_{n-1} - \frac{\lambda}{2}(1-r))$$

$$\tilde{\epsilon}_n = x_n - \tilde{x}_n = x_n - (rx_{n-1}^* - \frac{\lambda}{2}(1-r))$$

$$= x_n - \{r[\tilde{x}_{n-1} + q(\tilde{\epsilon}_{n-1})] - \frac{\lambda}{2}(1-r)\}$$

so that

$$\tilde{\epsilon}_n - \epsilon_n = r\, x_{n-1} - r\,[\tilde{x}_{n-1} + q(\tilde{\epsilon}_{n-1})] = r(\tilde{\epsilon}_{n-1} - q(\tilde{\epsilon}_{n-1}))$$

Since the processes are stationary we have that

$$E\{(\tilde{\epsilon}_n - \epsilon_n)^2\} = r^2 E\{(\tilde{\epsilon}_n - q(\tilde{\epsilon}_n))^2\} \tag{4.4}$$

so that as often conjectured, $\tilde{\tilde{\epsilon}}_n \cong \epsilon_n$ in a squared-error sense if the quantization error $E\{(\tilde{\epsilon}_n - q(\tilde{\epsilon}_n))^2\}$ is small. Using the fact that the densities are nearly symmetric about their mean so that with symmetric quantization $E(q(\tilde{\epsilon})) = 0 = E(\tilde{\epsilon})$ we have from above that

$$\sigma^2_{\tilde{\epsilon}} = E\{\tilde{\epsilon}_n^2\} = \sigma_\epsilon^2 + r^2 E\{(\tilde{\epsilon}_n - q(\tilde{\epsilon}_n))^2\} + 2r\,E\{\epsilon_n[\tilde{\epsilon}_{n-1} - q(\tilde{\epsilon}_{n-1})]\} \tag{4.5}$$

Intuitively, since $\tilde{\epsilon}_{n-1}$ and $q(\tilde{\epsilon}_{n-1})$

depend only on ϵ_{n-k} for $k \geq 1$ and are therefore nearly uncorrelated, the cross term above should be small so that

$$\sigma^2_{\tilde{\epsilon}} \cong \sigma_\epsilon^2 + r^2\, E\{(\tilde{\epsilon}_n - q(\tilde{\epsilon}_n))^2\} \tag{4.6}$$

The variance can be bounded above via the Cauchy inequality to obtain

$$\sigma^2_{\tilde{\epsilon}} \leq (\sigma_\epsilon + \quad r[E\{(\tilde{\epsilon}_n - q(\tilde{\epsilon}_n))^2\}]^{1/2})^2 \tag{4.7}$$

but this bound seems overly conservative and we instead use (4.6).

Since $\epsilon_n = (x_n - \lambda/2) - r(x_{n-1} - \lambda/2)$, the Gaussian approximation of the transition density of (2.5) implies that

$$f_{\epsilon_n | x_{n-1}}(\xi | x) = f_{x_n | x_{n-1}}(\xi - \lambda/2 + r(x - \lambda/2) | x)$$

$$\cong \frac{1}{\sqrt{2\pi\sigma_x^2(1-r^2)}} \exp\left[\frac{-1}{2\sigma_x^2(1-r^2)}\, \xi^2\right]. \tag{4.8}$$

If the quantization $E\{(\tilde{\epsilon}-q(\tilde{\epsilon}))^2\}$ is small enough, then $\tilde{\epsilon}_n$ should also be approximately Gaussian, but with possibly larger variance $\sigma_{\tilde{\epsilon}}^2$. This approximation, however, is not required in some of the analyses discussed and should be used with caution.

We first consider obtaining compression using uniform quantization followed by noiseless coding. We begin by noting that the errors are in general small so that with high probability $|\hat{\epsilon}_n| \leq \lambda/2$. Firstly, in all the observed earth scan data the jumps never exceed 3 volts in one sample. Secondly, if ϵ_n is approximately Gaussian with variance σ_ϵ^2, then $\Pr(|\epsilon_n| \geq \lambda/2) \cong 2Q(\lambda/2\sigma_\epsilon) \cong 2Q(3.3) \approx 0.$ a negligible amount. Thus if we uniformly quantize $\tilde{\epsilon}_n$ in the range $[-\lambda/2, \lambda/2]$ at rate R' we obtain via standard approximation that

$$E\{(\tilde{\epsilon}_n - q(\tilde{\epsilon}_n))^2\} \cong \frac{\lambda^2}{12} 2^{-2R'} \tag{4.9}$$

so that

$$E\{(x_n - x_n^*)^2\} \cong \frac{\lambda^2}{12} 2^{-2R'} \tag{4.10}$$

if x_n^* is reconstructed from the $q(\tilde{\epsilon}_n)$. We note that from (4.6) and (4.9) we have that

$$\sigma_{\tilde{\epsilon}}^2 \cong \sigma_\epsilon^2 + r^2 \frac{\lambda^2}{12} 2^{-2R'}$$

so that if $R' \geq 5$, the second term is negligible in comparison with the first so that $\sigma_{\tilde{\epsilon}}^2 \cong \sigma_\epsilon^2$ as desired.

We next attempt to achieve compression by noiseless encoding the quantized error sequence. Now, however, we wish to make use of the fact that it is the composite source v_n we wish to compress rather than x_n. To accomplish this we make a slight modification of the system. The principal difference between x_n and v_n is the presence of relatively rare but large jumps in the latter. Thus if we use the same prediction rule for v_n as we developed for x_n, we test to see if $|\tilde{\epsilon}_n| > \lambda/2$. If $|\tilde{\epsilon}_n| \leq \lambda/2$ we proceed as above and uniformly quantize $\tilde{\epsilon}_n$ on $[-\lambda/2, \lambda/2]$ and then noiselessly encoded the 6-bit symbol using a variable-length technique such as Huffman or Shannon-Fano coding. If $|\tilde{\epsilon}_n| > \lambda/2$, however, then we instead send a 6 bit quantized version of the actual data symbol

$$x_n \in [-\lambda, 0]$$

with an appropriate prefix to flag the presence of a data sample instead of an error

sample. This should almost never happen during an earth scan and happen only relatively rarely during the remainder of the period. The 6-bit word and its prefix are not noiselessly encoded as this likely provides little extra savings. The system described is depicted in Figure II.4.2. Note that the occasional transmission of $q(x_n)$ can only improve the average distortion by helping to minimize error buildup, but the rate will be slightly increased.

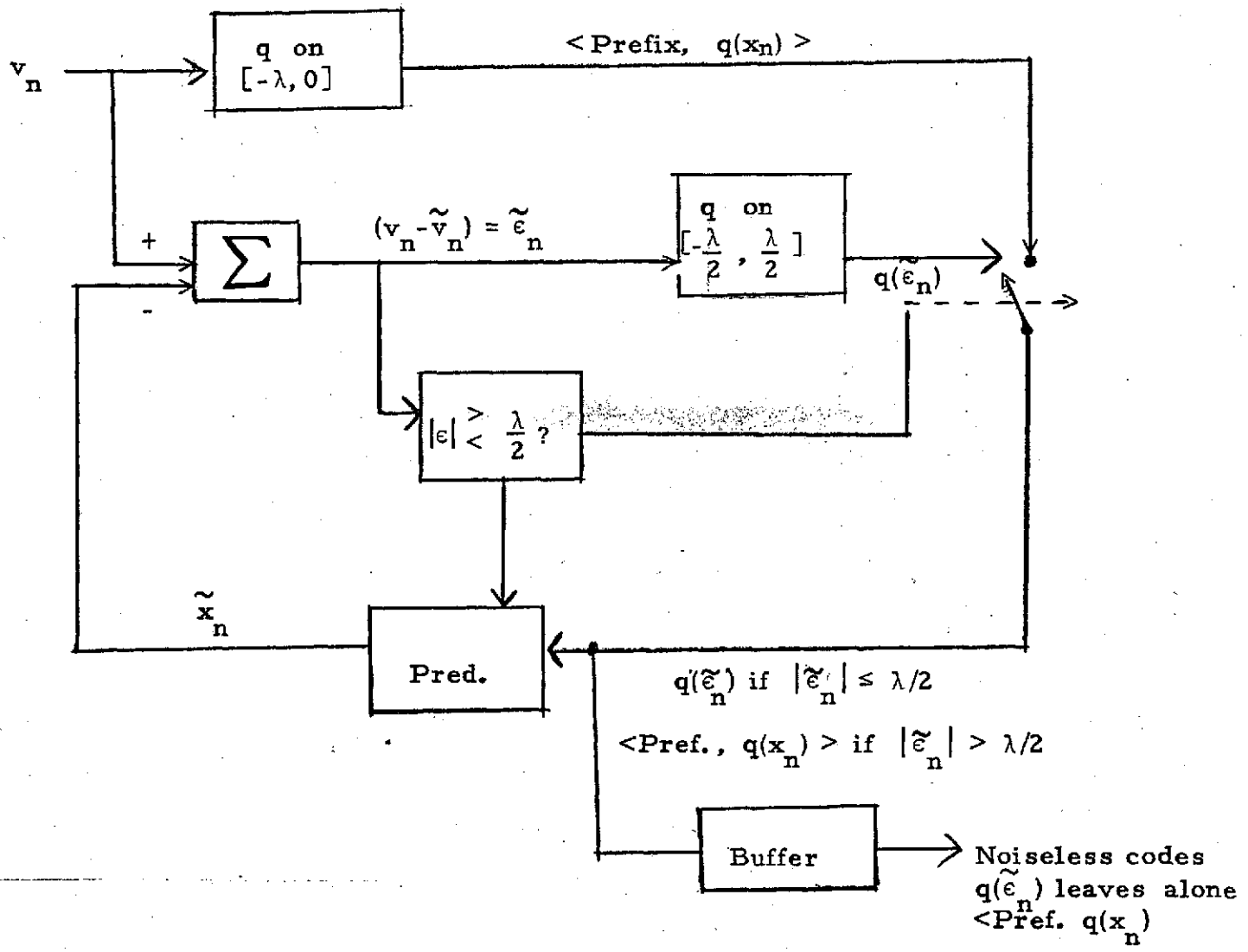

$$\tilde{x}_n = r[x_{n-1}^{*} + \lambda/2\,] - \lambda/2$$

$$x_{n-1}^{*} = \begin{cases} q(x_{n-1}) & q(x_{n-1}) \text{ sent last} \\ \tilde{x}_{n-1} + q(\tilde{\epsilon}_{n-1}) & q(\tilde{\epsilon}_{n-1}) \text{ sent last} \end{cases}$$

Figure II. 4. 2

For the modified system we have as before that

$$E\{(v_n - v_n^*)^2\} \tilde{=} \frac{\lambda^2}{12} 2^{-2R'} \tag{4.11}$$

We next consider the attainable bit rate in bits per symbol. Let N be a random variable denoting the number of bits required to encode each sample (either by quantizing the error or by quantizing the sample itself). The average rate in bits per symbol is then E[N] which by iterated expectation is

$$E[N] = E[N|v_n = x_n] \Pr[v_n = x_n] +$$

$$E[N|v_n = w_n] \Pr[v_n = w_n] + E[N|v_n = z_n] \Pr[v_n = z_n]$$

$$+ E[N|v_n = y_n] \Pr[v_n = y_n].$$

Let K denote the number of prefix bits attached when v_n is quantized (typically 4). We assume that a universal noiseless code is used, e.g., that empirical frequencies are used for the relative probabilities. Such a code will then work nearly optimally regardless of the subsource.

If $v_n = z_n$, either $\tilde{\epsilon}_n \tilde{=} 0$ or $\tilde{\epsilon}_n \tilde{=} 6$ so that

$$E[N|v_n = z_n] \tilde{=} (6+K) \Pr[\tilde{\epsilon}_n \geq \lambda/2 | v_n = z_n] = (6+K)/5$$

so that

$$E[N|u_n = z_n] \Pr[u_n = z_n]$$

$$\tilde{=} (6+K)(.2)(.02)$$

$$= (6+K)(.004)$$

To compute $E[N|v_n = x_n]$ we use a standard approximation which is accurate for moderate R':

$$H(q(\tilde{\epsilon}_n)|v_n = x_n) \tilde{=}$$

$$H(\tilde{\epsilon}_n|v_n = x_n) - \log_2 \lambda 2^{-R'}$$

$$= R' - \log_2 \lambda + H(\tilde{\epsilon}_n | v_n = x_n)$$

where H denotes the marginal differential entropy for $\tilde{\epsilon}_n$ (conditioned on $v_n = x_n$). H is bounded above (and approximated by) the differential entropy of a Gaussian variable with the same variance:

$$H(q(\tilde{\epsilon}_n) | v_n = x_n) \cong$$

$$R' - \log_2 \lambda + 1/2 \log_2 2\pi e \sigma^2_{\tilde{\epsilon}}$$

$$= R' + 1/2 \log_2 \frac{2\pi e \sigma^2_{\tilde{\epsilon}}}{\lambda^2}$$

$$\tilde{=} R' - .67 \qquad (4.12)$$

with $\sigma^2_{\tilde{\epsilon}} \tilde{=} .023 \lambda^2$

$$E[N|v_n = x_n] \Pr[u_n = x_n] \tilde{=} (R' - .674)(.6)$$

Using a similar approximation as above on w_n and the fact that $\Pr[|\tilde{\epsilon}_n| \geq .01 \,|\, v_n = w_n] \tilde{=} 0$ so that

$$\sigma^2_{\tilde{\epsilon}|w} \leq (.05)^2$$

$$H(q(\tilde{\epsilon}_n) | v_n = w_n) \leq$$

$$R' + 1/2 \log_2 2\pi e \sigma^2_{\tilde{\epsilon}|w} / \lambda^2 \tilde{=} R' - 5$$

so that

$$E[N|v_n = w_n] \Pr[v_n = w_n] \tilde{=} (R' - 5)(.04)$$

Finally, consider the subsource v_n of jumps. Jumps can occur no more often than once every 85 samples and of those jumps no more than 1/2 exceed $\lambda/2$, except for small λ. Thus

$$E\{N|v_n = y_n\} = E\{N|v_n = y_n, |\tilde{\epsilon}_n| > \lambda/2\} \cdot$$

$$\Pr\{|\tilde{\epsilon}_n| \geq \lambda/2 | v_n = y_n\} + E\{N | v_n = y_n, |\tilde{\epsilon}_n| \leq \lambda/2\} \cdot$$

$$\Pr\{|\tilde{\epsilon}_n| \leq \lambda/2 \mid v_n = y_n\}$$

$$= (R' + K)\, 1/2 \cdot 1/85 + E\{N | v_n = y_n, |\tilde{\epsilon}_n| \leq \lambda/2\} \times 1/2$$

$$\tilde{=} 1/2[H(\tilde{\epsilon}_n | v_n = y_n, |\tilde{\epsilon}_n|) + R' - \log_2 6]$$

for moderate K

$$\leqq [R' + 1/2 \log \frac{2\pi e \sigma^2_{\tilde{\epsilon}|v}}{\lambda^2}] 1/2$$

where

$$\sigma^2_{\tilde{\epsilon}|v} = E\{\tilde{\epsilon}_n^2 | v_n = y_n, |\epsilon_n| \leq \lambda/2$$

If

$$v_n = v_{n-1},\ |\tilde{\epsilon}_n| = |v_n - r v_{n-1}| = |1 - r|\, |v_{n-1}| \leq (.05)$$

and this occurs at least 84/85 of the time. If $v_n \neq v_{n-1}$, then there is a jump which is by assumption uniformly distributed over $[-\lambda/2, \lambda/2]$ so that

$$\sigma^2_{\tilde{\epsilon} \mid v} \tilde{=} (.05)^2 \ 84/85 + 1/2\ \lambda^2\ 1/85 \ \tilde{=}\ .001\lambda^2$$

so that

$$E\{N \mid v_n = y_n\} \leq 1/2\ \{R' + 1/2 \log \frac{2\pi e \sigma^2_{\tilde{\epsilon}}}{\lambda^2} = 1/2\ [R' - 5.9] = R'/2 - 3$$

Combining the previous relations we have for an efficient universal code that

$$E[N] \tilde{=} (6+K)\ (.004)$$

$$+ (R' - .674)\ (.6) + (R' - 5)\ (.04)$$

$$+ (R'/2 - 3)\ (.34)$$

The first and third terms are negligible (since so little time is spent in those subsources and since they are highly redundant). The expression becomes therefore

$$E[N] \tilde{=} (R' - .674)\ (.6) +$$

$$(R'/2 - 3)\ (.34)$$

The second term is likely somewhat conservative since a Gaussian bound was used and the data is quite non-Gaussian. The first term is likely more accurate since when x_n is in effect, $\tilde{\epsilon}_n$ is approximately Gaussian.

To summarize:

$$E\{x_n - x_n^*)^2\} = \frac{\lambda^2}{12} \; 2^{-R'}$$

$$R \tilde{=} E[N] \tilde{=} (R' - .674)\ (.6) + (\frac{R'}{2} - 3)\ (.34)$$

where a buffer of roughy (150) x (100) samples is required so that the output bit stream will have rate $\tilde{=}$R. In particular, for R' = 6 bits and λ = 6 so that the entire range is quantized,

$$E[(x_n - x_n^*)^2] = 7.32 \times 10^{-4}$$

as desired, and

$$R \tilde{=} 3.20$$

The same compression can be achieved by synchronizing on the earth scan and transmitting only that data with the calibration and telemetry data multiplexed in. In this case, further compression can be achieved by quantizing a narrower range of values. Empirical studies indicate that the earth scan values are confined to approximately 25% of the total possible range so that R' = R - 2 bits is adequate. Combined with the variable length coding factor, an overall reduction of approximately 3 bits is then possible for R = 6 to 8 bits.

Data compression with predictive quantization can also be achieved using nonuniform quantization of the error sequence. This scheme has the advantage of being fixed rate, but the disadvantage of depending crucially on the model for choosing the quantization intervals. The noiseless coding, however, can adapt to the varying subsources. In addition, in some calculations involving the x_n subsource alone, the nonuniform quantizer appeared comparable but slightly inferior to the noiseless-coded scheme and hence this system was not studied further.